Journal of Fluorescence
https://doi.org/10.1007/s10895-020-02524-z

ORIGINAL ARTICLE

A Fluorescence Resonance Energy Transfer Biosensor Based on Graphene Quantum Dots and Protoporphyrin IX for the Detection of Melamine

Gao Xue[1] · Ma Zhiying[1] · Liu Xiuying[1] · Tang Lijun[1] · Li Jianrong[1]

Received: 2 January 2020 / Accepted: 9 March 2020

Abstract

Graphene quantum dots (GQDs), which have high photostability, anti-photobleaching and scintillation, good biocompatibility and low toxicity, are important member of the fluorescent material family, and have attracted extensive research interest. In this paper, a fluorescence resonance energy transfer (FRET) biosensor based on protoporphyrin IX (PpIX) and GQDs was developed for melamine detection. PpIX was bound to the surface of GQDs to produce self-assembled nanosensors, and a FRET process occurred between GQDs and PpIX. However, due to the combination of melamine and PpIX, the FRET process was shut down in the presence of melamine. The FRET system could quickly and accurately detect melamine with a detection range of 1.0×10^{-8} to 2.0×10^{-6} mol/L based on the fluorescence intensity ratio of PpIX and GQDs, and the detection limit was 3.6×10^{-9} mol/L. This method obtained satisfactory results when it was employed to the determination of melamine in milk samples.

Keywords Graphene quantum dots · Protoporphyrin IX · FRET · Melamine

Introduction

Graphene quantum dots (GQDs), as the new nanometer material, have made up for the defects of the traditional detection technology, and make great achievements in modern analytical methods. GQDs have many advantages, such as strong photostability, high chemical inertness, tunable photoluminescence, good solubility, high biocompatibility, small molecular weight and easy functionalization, which are very outstanding compared with traditional fluorescent probes, such as semiconductor quantum dots (QDs) and organic fluorescent clusters [1–5]. Because of these characteristics, GQDs have been widely used in photocatalysis, fluorescence bio-imaging, drug delivery, biosensors and chemical sensors, as well as photosensitizers in photodynamic therapy, and become a potential substitute for semiconductor quantum dots [6–9]. Under the influence of delocalized π electrons, GQDs interact with a variety of aromatic molecules by noncovalent π-π stacking. The hybrid supramolecular assembly of GQDs and organic macrocycles (such as porphyrins) have broad research prospects, and will promote these applications in related fields. In recent years, QDs have become ideal donor materials in fluorescence resonance energy transfer (FRET) bioanalysis technology and been widely studied and applied in this field, due to their excellent photostability and highly tunable emission properties [10–16].

Protoporphyrin (PpIX) is a photosensitizer, whose sensitivity to light is made for use in therapy against different forms of cancer [17]. This fluorescent molecule is used as a photosensitizer in photodynamic therapy (PDT), because it can produce singlet oxygen species and can form free radicals that result in cellular damage to various organelles [18]. As a kind of macrocyclic organic molecules with a wide range of delocalized π electrons, the binding and catalytic properties of PpIX mainly depend on the binding of metals with central nitrogen atoms

Electronic supplementary material The online version of this article (https://doi.org/10.1007/s10895-020-02524-z) contains supplementary material, which is available to authorized users.

✉ Gao Xue
huaxue_gaoxue@126.com

✉ Li Jianrong
lijr6491@163.com

[1] College of Food Science and Technology, National & Local Joint Engineering Research Center of Storage, Processing and Safety Control Technology for Fresh Agricultural and Aquatic Products, Food Safety Key Lab of Liaoning Province, The Fresh Food Storage, Processing Technology Research Institute of Liaoning Provincial Universities, Bohai University, Jinzhou, China

Published online: 12 September 2020

by coordination and the change of surrounding substituent. PpIX is an important macrocyclic compound with large conjugated π-electron system, which can be used in the assembly of donor-acceptor materials in molecular electronics and photovoltaic devices [19].

1,3,5-triazine-2,4,6-triamine ($C_3H_6N_6$), called melamine, is an organic chemical used to produce melamine formaldehyde resins. It is mainly used in the manufacturing of plastics, adhesives, laminates, and cooking utensils [20]. The insatiable profit-seekers mixed melamine into milk, which made the protein content measured by Kjeldahl method higher [21], thereby obtaining higher prices in the milk market and misleading the consumers. If people often absorb melamine through milk, it will cause kidney damage and more other types of health problems. Therefore, a rapid and sensitive analytical method for determination of melamine in food products is very imminent to the whole society. Several detection methods for melamine had been reported such as mass spectrometry (MS) [22], surface enhanced Raman scattering (SERS) sensor [23], matrix-assisted laser desorption/ionization mass spectrometry (MALDI-MS) [24], near-infrared reflectance spectroscopy (NIRS) [25], electrochemical biosensor [26], and colorimetry [27]. Compared with the above analytical techniques, visual inspection has led the development of melamine detection technology. It has the advantages of simplicity, cheapness, and can achieve the real-time analysis of the test samples with high sensitivity and high selectivity. Although several fluorescence methods for melamine detection have been reported, as far as we know, few reports have been reported on the use of FRET method for melamine detection [28], and few reports have been reported on the use of GQDs–PpIX FRET system for melamine detection in milk.

In this paper, a novel, effective and rapid method based on t the FRET system between GQDs and PpIX was put forward to detect melamine from milk. Fluorescence quenching of GQDs in the presence of PpIX indicated that the FRET from GQDs to PpIX. However, due to the combination of PpIX and melamine, the FRET process was switched off after adding melamine. Therefore, melamine detection can be accomplished by the new FRET model and GQDs–PpIX probe. Moreover, the selectivity and sensitivity of the sensors based on the FRET system were verified by the actual sample tests.

Materials and Methods

Materials and Apparatus

All the reagents, including phosphorus pentoxide (P_2O_5, ≥98.0%), N,N-Dimethylformamide (DMF) and graphite powder (325 mech, 99.95% metal basis) (Aladdin, Shanghai, China); potassium peroxydisulfate ($K_2S_2O_8$) (Fuchen Chemicals, Tianjin, China); potassium permanganate ($KMnO_4$) and hydrogen peroxide (30%) (Tianli Chemicals, Tianjin, China); concentrated sulfuric acid (H_2SO_4, 98%) (Jinzhou Chemicals, Liaoning, China); and melamine (Beijing Chemicals, Beijing, China), were analytically pure and used without further purification. Raw milk was provided by a local grocery store in authors' university. Deionized water with a resistivity of no less than18 MΩ/cm was used throughout the experiments. The pH values were obtained using apH meter (PHS-3C, Tuopu, Hangzhou, China). The fluorescence spectra of samples were measured by a spectra fluorophotometer (Fluoromax-4NIR, HORIBA Jobin Yvon, New Jersey, USA) equipped with a quartz cuvette (1 cm path-length).

GQDs Preparation

Graphene oxide (GO) was prepared by the Hummers method with slightly modification compared with the previous report [29]. GQDs were further prepared using GO as the raw material by one-step solvothermal method. First, 810 mg GO was mixed with 60 mL DMF in the ultrasound condition (120 W, 53 kHz) and stirred for 90 min. Then, the mixture was poured into a Teflon-lined autoclave with the volume of 50 mL. The reaction was conducted at 200 °C for a duration of 8 h. After that, the obtained mixture was naturally cooled to the room temperature and filtered through a membrane of 0.22 μm. The brown filtrate contained GQDs dispersing in the DMF. The concentration of GQDs was 2.18 mg/mL.

Fluorescence Detection of Melamine

A general FRET-based analysis of melamine was carried out as follows. Known amounts of GQDs DMF dispersion and PpIX were transferred into 2 mL centrifuge tubes containing various amounts of melamine. Then PBS (pH = 7.4) was added to dilute the mixture to 2.0 mL, and the mixture was agitated for 20 min at room temperature. Thereafter, the fluorescence emission spectra over 420 to 780 nm with an excitation of 400 nm were recorded. The relationship between I_{PpIX}/I_{GQDs} (where I_{PpIX} and I_{GQDs} referred to the fluorescence intensities of PpIX and GQDs, respectively) and melamine concentration was plotted in the calibration curve.

Detection of Melamine in Actual Samples

In the actual sample detection, milk samples were treated in prior to analysis according to the reported study [30]. Firstly, 5 mL of raw milk was mixed with 1 mL of 2 mol/L trichloroacetic acid. Then, the protein was precipitated from the solution after ultrasonic treatment for 10 min. The supernatant was separated by centrifugation at 10,000 rpm for 10 min, and neutralized with 1 mol/L NaOH solution until the pH value

reached 7.4. Afterwards, a 0.45 μm filter was used to make the obtained supernatant clear, and ultrapure water was added into the supernatant to dilute it to an appropriate concentration within the detection range [27]. For real sample analysis, the same pretreatment was applied to melamine (known concentration) milk sample.

Results and Discussion

Optical Characteristics of GQDs and PpIX

The physical properties of donor and acceptor, especially the degree of overlap of energy levels of the donor and acceptor, have an important influence on energy transfer efficiency. The absorption and emission spectra of GQDs and PpIX were shown in Fig. 1. The emission spectra of GQDs overlapped obviously with the absorption spectra of PpIX, indicating the energy transfer from GQDs and PpIX. On the contrary, it was impossible to transfer energy from PpIX to GQDs, mainly because of the inconsistency of energy between them, and the lack of overlap between the absorption spectrum of GQDs and the emission spectrum of PpIX. Consequently, 400 nm excitation light was chosen to excite the donor, ensuring the well stimulation of GQDs and no stimulation of PpIX, which effectively reduced the interference caused by direct excitation of the receptor.

FRET-Based Compound of GQDs and PpIX

It was very important to fully understand how GQDs and PpIX were attached with each other for the study of GQDs-PpIX system. Upon mixing the dilute aqueous solutions of GQDs with PpIX, the complexes were formed by the electrostatic association of PpIX on the surface of GQDs. In fact, the acidification of H_2SO_4 gave a positive charge to the PpIX molecule, and the carboxylic acid group on the surface gave a negative charge to the GQDs. As a result, the negatively charged GQDs and positively charged PpIX molecules became very close under electrostatic interaction. As shown in Fig. 2, the fluorescence intensity of GQDs gradually decreased and the fluorescence intensity of PpIX increased along with the increasing concentrations of PpIX. In this paper, the quenching of GQDs fluorescence via energy transfer was studied by the distribution of pyridine ring in mesoscopic position. According to a previous study, the QD/porphyrin conjugate was formed by two cis pyridyl rings facilitate porphyrin binding to the QDs surface [31]. FRET resulted in the enhancement of the association effect of PpIX emission on GQDs. As an important part of these assemblies, GQDs played the role of antenna to absorb photons. Energy was passed from the GQDs donor to PpIX acceptor by the FRET mechanism.

Most of the experiments involving FRET need to calculate the energy transfer efficiency (E) to obtain relatively accurate results of the efficiency of energy transfer [32, 33]. E can be measured and calculated as follows:

$$E = 1 - I/I_0 \quad (1)$$

where I and I_0 refer to the fluorescence intensities of the donors (GQDs) in the presence and absence of the acceptor (PpIX), respectively.

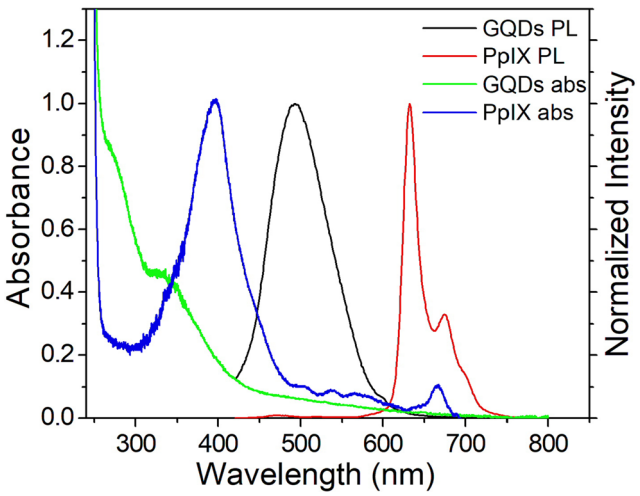

Fig. 1 Normalized absorption and fluorescence spectrum of GQDs and PpIX solution

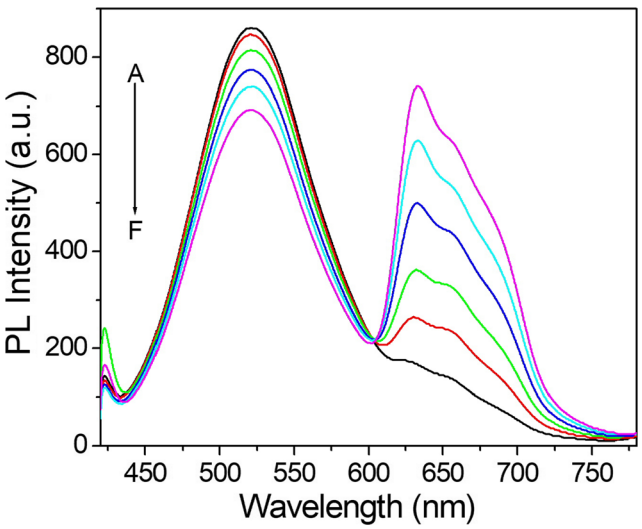

Fig. 2 The fluorescence spectra of the FRET system with different concentrations of PpIX, A-F: 2.5×10^{-8}, 5.0×10^{-7}, 1.0×10^{-7}, 2.0×10^{-7}, 3.0×10^{-7} and 4.0×10^{-7} mol/L, respectively

The energy transfer efficiency depends on the distance between the donor-acceptor pair, and the dependence relationship could be expressed as follows:

$$E = R_0{}^6/\left(R_0{}^6 + R^6\right) \quad (2)$$

where R is the actual distance between donor–acceptor pair, and R_0 is the critical distance with the energy transfers efficiency of 50%, which could be calculated as follows:

$$R_0{}^6 = 8.8 \times 10^{-25} K^2 n^{-4} \Phi J(\lambda) \quad (3)$$

where K^2 is 2/3, which means the spatial orientation factor. n is 1.336, which means the refraction index. Φ is 23.6% in our experiments, measured using the ethanol solution of rhodamine 6G as the reference standard, which refers to the quantum yield of GQDs. J(λ) is the spectral overlap integral, which can be calculated as follows:

$$J(\lambda) = \left[\sum I(\lambda)\varepsilon(\lambda)\,\lambda^4 \Delta\lambda\right]/\left[\sum I(\lambda)\,\Delta\lambda\right] \quad (4)$$

where λ refers to the wavelength, I(λ) refers to the fluorescence intensity of the fluorescence donor, ε(λ) refers to the molar absorption coefficient of the acceptor with the unit of L/mol/cm. Figure 1 exhibits the overlap between the fluorescence emission spectrum of PpIX and the absorption spectrum of GQDs. Hence, J(λ) could be calculated by Eq. (4) from the FRET spectrum with the wavelength range of 420–780 nm, and J(λ) is calculated to be 1.928×10^{-13} cm^3 L/mol. According to Eq. (3), R_0 obtains the value of 4.51 nm.

In this paper, according to Eq. (1), the energy transfer efficiency could be up to 80.0%. According to Eq. (2), there was a distance of 3.57 nm between PpIX and GQDs, which was small enough to make the FRET occur. These results indicated the high probability of energy transfer from GQDs to PpIX.

Detection of Melamine

We investigated the effect of time on melamine detection. As shown in Fig. 3, with the increase of reaction time, the fluorescence intensity ratio I_{PpIX}/I_{GQDs} gradually decreased in the first 20 min. The I_{PpIX}/I_{GQDs} ratio tended to be constant from 20 to 35 min, which indicated that the reaction terminated after the reaction lasting for 20 min. As a result, the best reaction time was 20 min in this experiment.

As mentioned above, GQDs and PpIX can form FRET donor–acceptor assemblies, resulting in effective quenching of GQDs emission. The existence of melamine can destroy the GQDs-PpIX assembly, which was because that melamine and PpIX molecules can form an association system, and GQDs were separated after the combination of melamine and PpIX molecules. The structures of PpIX and melamine were shown in Fig. S1 (see Supplementary Materials). Since the surface of PpIX containing carboxyl groups (–COOH) appears as negative charge, when the pH value of the entire solution is kept to about 7.4. The carboxyl group on the surface of PpIX can interact with the amino group (-NH_2) contained in melamine to form hydrogen bond. Electrostatic and hydrogen bonding are two important factors for melamine to bind to the surface of PpIX. From this point of view, the aggregation of PpIX is promoted by the presence of melamine. As mentioned above, hydrogen bond will be formed between the amino group of melamine and the carboxyl group of PpIX, and the self-assembly of PpIX can be carried out under the action of hydrogen bond. This self-assembly depends on π-π interaction, which is the net result of π-σ interaction excluding π-π repulsion [34]. This π-π interaction exists between the aromatic PpIX macrocycles and in the hydrogen bonds between amines of the melamine and electrostatic attractions and carboxyl groups of PpIX [35].

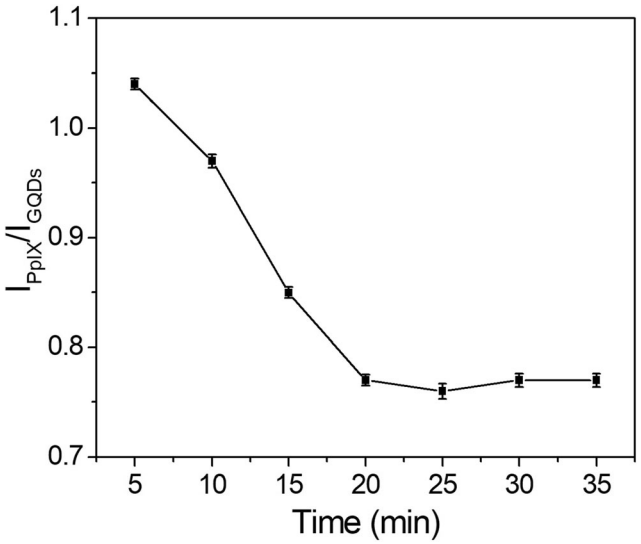

Fig. 3 The relationship between the fluorescence intensity ratio I_{PpIX}/I_{GQDs} (I_{PpIX} and I_{GQDs} refer to the fluorescence intensity of PpIX and GQDs, respectively) and the incubation time in the presence of melamine

The fluorescence spectra of the GQDs-PpIX FRET system with the addition of various amounts of melamine at pH = 7.4 were recorded. Figure 4 illustrated plots of I_{PpIX}/I_{GQDs} versus the concentration of melamine. Obviously, the efficiency of the FRET system was significantly decreased by the presence of melamine. In the melamine concentration range of 1.0×10^{-8}-2.0×10^{-6} mol/L, there was a good linearity. On the basis of three times of standard deviation of the blank signal for melamine, a limit of detection (LOD) of 3.6×10^{-9} mol/L was obtained. The linear regression equation was $I_{PpIX}/I_{GQDs} = -1.088–0.446\log C_{melamine}$ (mol/L), and the correlation coefficient (R^2) was 0.998.

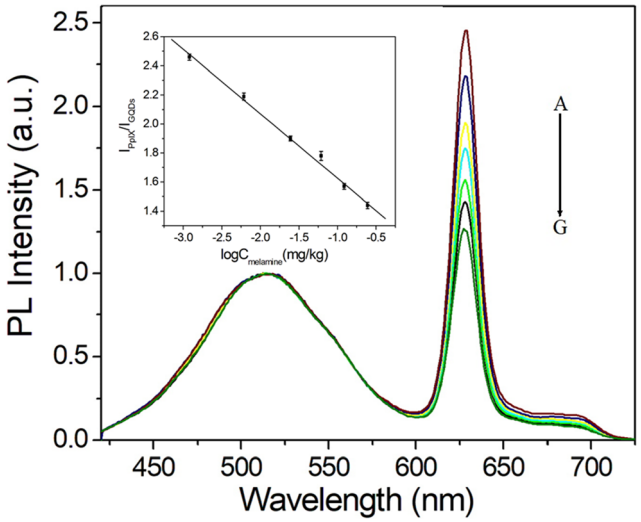

Fig. 4 The fluorescence spectra of the GQDs-PpIX FRET system in the presence of various concentrations of melamine, A-P represents the concentration of melamine of 0, 2.0×10^{-6}, 5.0×10^{-7}, 2.0×10^{-7}, 5.0×10^{-8} and 1.0×10^{-8} mol/L, respectively. The inset shows the relationship between I_{PpIX}/I_{GQDs} (I_{PpIX} and I_{GQDs} refer to the fluorescence intensity of PpIX and GQDs, respectively) and the concentration of melamine

Interference Study

Usually, some coexisting substances may affect the detection of actual samples. To explore the precision of this method, solutions with the melamine concentration of 1.0×10^{-7} mol/L and different potential sources of interferences were tested under the same conditions. Table 1 showed the interference effect of some common mental ions, glycine, glucose, vitamin C and bovine serum albumin (BSA) on the determination of melamine. The relative error was less than (±5.0%) which proved that the substance had no interference in the detection of melamine. As shown in Table 1, the tolerable concentration ratios of the coexisting substances to 1.0×10^{-7} mol/L melamine were over 10^4-fold for KCl, NaCl, vitamin C, glycine, BSA and glucose, 500-fold for $Mg(NO_3)_2$ and $CaCl_2$. The experimental results showed that these coexisting substances had little interference with the detection of melamine. Therefore, this method was proved to have high selectivity for detecting melamine.

Table 1 The interference of coexisting substances on the determination of melamine (0.0122 mg/kg)

Coexisting substance	Tolerable Concentration (mg/kg)	Molar Ratio	ΔI/I (%)
KCl	122	10^4	−4.8
NaCl	122	10^4	−3.6
$Mg(NO_3)_2$	6.1	500	2
$CaCl_2$	6.1	500	−5
Glycine	122	10^4	4.8
Vitamin C	122	10^4	4.7
BSA	122	10^4	−1
Glucose	122	10^4	−1.3

Table 2 Determination of melamine in milk samples

Sample	Added (mg/kg)	Found (mg/kg)	Recovery (%)	RSD (%, n = 3)
Milk	0.00	0.00	-	-
	0.024	0.027	112	1.1
	0.061	0.066	107	0.9

Analysis of Melamine in Actual Samples

Melamine in three different milk samples was detected by the FRET system to verify the applicability of this method in the actual sample detection. In conventional detection techniques, the melamine needed complex processing steps and extraction procedures, which were time- and cost-consuming and liable to pesticide loss. In our experiment, the pretreatment as preciously described in Experimental section was applied to milk samples, avoiding the use of organic solvents and tedious preconcentration steps. In the actual detection, the processed milk sample solution was diluted for testing until the desired concentration was achieved. As shown in Table 2, the detection recoveries of melamine in cucumber was 107%–112%, with the relative standard deviation (RSD, $n = 3$) less than 1.4%. Results showed that this method had practical application value in detecting melamine in actual samples. The precision of the biosensor to detect melamine in milk samples was acceptable. The results were more reliable and satisfactory than other detection methods.

Conclusion

In conclusion, a FRET system for the sensitive, rapid, and selective detection method of melamine was proposed in this study based on GQDs and PpIX. Compared with the methods reported in the past, this method is simple and efficient, and has many advantages, such as good repeatability, constant recovery, high accuracy and good linear working range. In the proposed sensing strategy, the minimum detection concentration of melamine does not exceed the safety limit of melamine in dairy products, which meets the detection requirements. Satisfactory results were obtained when the proposed method was applied to detecting melamine in actual samples.

Acknowledgements This work was financially supported by a grant from the National Natural Science Foundation of China (No. 31501564), the central government guides local science and technology development special funds project (No. 2018107005), the Team Support Program for the Taishan Scholar of Blue Industry leading personnel of shandong Province of China (LZBZ2015-19).

References

1. Sk MA, Ananthanarayanan A, Huang L, Lim KH, Chen P (2014) Revealing the tunable photoluminescence properties of graphene quantum dots. J Mater Chem C 2:6954–6960
2. Bacon M, Bradley SJ, Nann T (2014) Graphene quantum dots. Part Part Syst Charact 31:415–428
3. Wang D, Chen JF, Dai L (2015) Recent advances in graphene quantum dots for fluorescence bioimaging from cells through tissues to animals. Part Part Syst Charact 32:515–523
4. Zheng XT, Ananthanarayanan A, Luo KQ, Chen P (2015) Glowing graphene quantum dots and carbon dots: properties, syntheses, and biological applications. Small 11:1620–1636
5. Ananthanarayanan A, Wang Y, Routh P, Sk MA, Than A, Lin M, Zhang J, Chen J, Sun HD, Chen P (2015) Nitrogen and phosphorus co-doped graphene quantum dots: synthesis from adenosine triphosphate, optical properties, and cellular imaging. Nanoscale 7: 8159–8165
6. Fan Z, Li S, Yuan F, Fan L (2015) Fluorescent graphene quantum dots for biosensing and bioimaging. RSC Adv 5:19773–19789
7. Achadu OJ, Uddin I, Nyokong T (2016) The interaction of graphene quantum dots grafted with polyethyleneimine and Au@Ag nanoparticles: application as fluorescence "turn on" nanoprobes. J Photochem Photobiol A Chem 324:96–105
8. Qu D, Zheng M, Du P, Zhou Y, Zhang L, Li D, Tan H, Zhao Z, Xied Z, Sun Z (2013) Highly luminescent S, N co-doped graphene quantum dots with broad visible absorption bands for visible light photocatalysts. Nanoscale 5:12272–12277
9. Ge J, Lan M, Zhou B, Liu W, Guo L, Wang H, Jia Q, Niu G, Huang X, Zhou H, Meng X, Wang P, Lee CS, Zhang W, Han X (2014) A graphene quantum dot photodynamic therapy agent with high singlet oxygen generation. Nat Commun 5:4596
10. Willard DM, Carillo LL, Jung J, Orden AV (2001) CdSe−ZnS quantum dots as resonance energy transfer donors in a model protein−protein binding assay. Nano Lett 1:469–474
11. Mamedova NN, Kotov NA (2001) Albumin−CdTe nanoparticle bioconjugates: preparation, structure, and interunit energy transfer with antenna effect. Nano Lett 1:281–286
12. Kagan CR, Murray CB, Bawendi MG (1996) Long-range resonance energy transfer of electronic excitations in close-packed cdse quantum-dot solids. Phys Rev B 54:8633–8643
13. Clapp AR, Medintz IL, Mauro JM, Fisher BR, Bawendi MG, Mattoussi H (2004) Fluorescence resonance energy transfer between quantum dot donors and dye-labeled protein acceptors. J Am Chem Soc 126:301–310
14. Medintz IL, Clapp AR, Mattoussi H, Goldman ER, Fisher B, Mauro JM (2003) Self-assembled nanoscale biosensors based on quantum dot FRET donors. Nat Mater 2:630–638
15. Zhang CY, Yeh HC, Kuroko MT, Wang TH (2005) Single-quantum-dot-based DNA nanosensor. Nat Mater 4:826–831
16. Alivisatos P (2000) Colloidal quantum dots. From scaling laws to biological applications. Pure Appl Chem 72:3–5
17. Peng Q, Warloe T, Berg K, Moan J, Kongshaug M, Giercksky KE, Nesland JM (1997) 5-Aminolevulinic acid-based photodynamic therapy. Clinical research and future challenges. Cancer 79:2282–2308
18. Kormeili T, Yamauchi PS, Lowe NJ (2004) Topical photodynamic therapy in clinical dermatology. Br J Dermatol 150:1061–1069
19. Dillon AC (2010) Carbon nanotubes for Photoconversion and electrical energy storage. Chem Rev 110:6856–6872
20. Rovina K, Siddiquee S (2015) A review of recent advances in melamine detection techniques. J Food Compos Anal 43:25–38
21. Li J, Mei F, Li WY, He XW, Zhang YK (2008) Study on the fluorescence resonance energy transfer between CdTe QDs and butyl-rhodamine B in the presence of CTMAB and its application on the detection of Hg(II). Spectrochimica Acta Part A-Molecul Biomolecul Spectroscop 70:811–817
22. Yang S, Ding J, Zheng J, Hu B, Li J, Chen H, Zhou Z, Qiao X (2009) Detection of melamine in milk products by surface desorption atmospheric pressure chemical ionization mass spectrometry. Anal Chem 81:2426–2436
23. Kim A, Barcelo SJ, Williams RS, Li Z (2012) Melamine sensing in milk products by using surface enhanced Raman scattering. Anal Chem 84:9303–9309
24. Tang HW, Ng KM, Chui SSY, Che CM, Lam CW, Yuen KY, Siu TS, Lan LCL, Che XY (2009) Analysis of melamine cyanurate in urine using matrix-assisted laser desorption/ionization mass spectrometry. Anal Chem 81:3676–3682
25. Haughey SA, King PG, Malechaux A, Elliott CT (2015) The use of handheld near-infrared reflectance spectroscopy (NIRS) for the proximate analysis of poultry feed and to detect melamine adulteration of soya bean meal. Anal Methods 7:181–186
26. Fu C, Liu C, Li Y, Guo Y, Luo F, Wang P, Guo L, Qiu B, Lin Z (2016) Homogeneous electrochemical biosensor for melamine based on DNA triplex structure and exonuclease III-assisted recycling amplification. Anal Chem 88:10176–10182
27. Ding N, Yan N, Ren C, Chen X (2010) Colorimetric determination of melamine in dairy products by Fe_3O_4 magnetic nanoparticles-H_2O_2-ABTS detection system. Anal Chem 82:5897–5899
28. Tang GC, Du LP, Su XG (2013) Detection of melamine based on the fluorescence resonance energy transfer between CdTe QDs and Rhodamine B. Food Chem 141:4060–4065
29. Gao X, Zhang B, Zhang Q, Tang YW, Liu XY, Li JR (2018) The influence of combination mode on the structure and properties of graphene quantum dot-porphyrin composites. Colloids Surf B: Biointerfaces 172:207–212
30. Yin M, Zhao L, Wei Q, Li H (2015) RSC Adv 5:32897–32901
31. Lemon CM, Elizabeth K, Bawendi MG, Nocera DG (2013) Two-photon oxygen sensing with quantum dot-porphyrin conjugates. Inorg Chem 52:10394–10406
32. Li J, Mei F, Li WY, He XW, Zhang YK (2008) Study on the fluorescence resonance energy transfer between CdTe QDs and butyl-rhodamine B in the presence of CB and its application on the detection of Hg(II). Spectrochimica Acta Part A-Molecul Biomolecul Spectroscop 70:811–817
33. Clapp AR, Medintz IL, Mattoussi H (2006) Förster resonance energy transfer investigation using quantum-dot fluorophores. Chem Phys Chem 7:47–57
34. Hunter CA, Sanders JKM (1990) The nature of .pi.-.pi. interactions. J Am Chem Soc 112:5525–5534
35. Bhosale RS, La DD, Kobaisi MA, Bhosale SV, Bhosale SV (2017) Melamine and spermine mediated supramolecular self-assembly of octaphosphonate tetraphenyl porphyrin. ChemistrySelect 2:1573–1577